*Lighting Res. Technol.* 2025; **XX**: 1–27

The Society of Light and Lighting

# Methodology to modify and adapt the standardised spectral power distributions for daylight to account for geographical, seasonal and diurnal variations for practical applications

**M Knoop**[a], **P Balakrishnan**[a], **UJ Błaszczak**[b], **AK Diakite-Kortlever**[a], **D Dumortier**[c], **J Hernández-Andrés**[d], **M Inanici**[e], **P Kenny**[f], **M Maskarenj**[g], **P O'Mahoney**[h], **C Pierson**[i], **F Rudawski**[a] and **A Thorseth**[j]

[a]Chair of Lighting Technology, Technische Universität Berlin, Berlin, Germany
[b]Department of Photonics, Electronics and Lighting Technology, Bialystok University of Technology, Bialystok, Poland
[c]ENTPE, LTDS, Vaulx-en-Velin, France
[d]Departamento de Óptica, Universidad de Granada, Granada, Spain
[e]Department of Architecture, University of Washington, Seattle, WA, USA
[f]School of Architecture, Planning and Environmental Policy, University College Dublin, Dublin, Ireland
[g]Louvain Research Institute for Landscape, Architecture, Built Environment, Université catholique de Louvain, Louvain-la-Neuve, Belgium
[h]UK Health Security Agency, Oxford, UK
[i]School of Civil and Construction Engineering, Oregon State University, Corvallis, OR, USA
[j]Department of Electrical and Photonics Engineering, Technical University of Denmark, DTU Electro, Roskilde, Denmark

Received 7 February 2024; Revised 26 January 2025; Accepted 30 January 2025

In recent years, the spectral properties of solar radiation and daylight have become increasingly important in lighting design and research, and various approaches to implement these have been applied. This paper proposes to modify and adapt the CIE reconstruction method, a procedure developed in the early 1960s to define standardised spectral power distributions (SPDs) of daylight, for this purpose. The CIE D Illuminants resulting from the reconstruction procedure are widely used for standardisation purposes but are based on a smaller number of measurements and do not consider geographical, seasonal and diurnal variations. In order to be able to use the CIE reconstruction method specifically in daylight planning, research and application, a technical committee of the CIE has launched a worldwide measurement campaign to collect spectral daylight measurements. The aim of the committee is to formulate a customised reconstruction method that more accurately reflects the local SPDs of daylight. This paper contributes to the discourse on the improvement of daylight estimation methods and emphasises the importance of accurate daylight data in various scientific and practical contexts.

Address for correspondence: M Knoop, Chair of Lighting Technology, Technische Universität Berlin, Einsteinufer 19, Sekr. E6, Berlin 10587, Germany.
E-mail: martine.knoop@tu-berlin.de

 10.1177/14771535251322386

## 1. Introduction

This paper presents a methodology to create representative spectral power distributions (SPDs) for daylight conditions, considering geographical, seasonal and diurnal variations. These SPDs can be used for daylighting research, design and application purposes. It builds upon the use of the spectral properties of solar radiation and daylight in various disciplines, as in recent years, work with this type of data has increased significantly. This includes work in the development of solar technology, lighting design to support human health and lighting optimisation for plant growth. This paper gives a brief overview of the use of spectral measurements and models and standardised SPDs. A larger number of associated uses of spectral characteristics of solar radiation or daylight can be found in the introduction of an overview paper of Gueymard.[1]

### 1.1 Use of spectral measurements and models of solar radiation and daylight

Spectral solar radiation measurements conducted at weather and observation centres by the *atmospheric science* community are, for example, being used to study atmospheric composition (e.g. in the Network for the Detection of Atmospheric Composition Change (NDACC),[2] and its impact on our climate, ecosystems and human health. The ground-based characterisation is typically done using a spectroradiometer,[3] a sensor or dosimeter to measure solar radiation in specific UV wavelength bands,[4] or a multidirectional spectroradiometer.[5] Within this field of expertise, radiative transfer models, such as libRadtran,[6] SBDART[7] and MODTRAN,[8] were developed to simulate the spectrally resolved transfer of extra-terrestrial radiation through the atmosphere.

Within the area of *flora and fauna, agriculture and forestry*, spectral daylight data can be employed in such fields as agriculture and horticulture, photosynthesis, crop and forest productivity and the terrestrial ecosystem. The spectrum of light influences photosynthetic and photomorphogenic processes in plant growth, which is of interest in predicting agricultural yield, as well as in spectral-tuning of complementary electric lighting for providing daily light integration in artificial and semi-artificial zones such as greenhouses. Thus, local daylight measurements,[9,10] or simulations with standardised SPDs of daylight as proposed by Ashdown,[11] could increase prediction accuracy as well as better design for such lighting systems. Additionally, soil characterisation in the field can be improved with knowledge of the spectral composition of daylight.[12]

The field of *computer graphics*, more specifically the domain that provides outdoor lighting conditions for product visualisation, the movie and gaming industry, as well as autonomous vehicle sensor training, benefits from simulated spectral sky conditions. Various approaches are utilised in the field to generate spectral sky conditions, including image-based lighting,[13,14] sky models using approximations and lookup tables[15] or fitted analytic sky models using atmospheric details.[16–19] These approaches provide a fast and realistic rendering of static and dynamic outdoor daylighting conditions.

In discipline-specific studies of *solar energy*, spectral characteristics of solar radiation are typically derived from solar measurements, satellite-based models, numerical weather prediction models, radiative transfer models and reference solar spectra (total global, direct and diffuse) to determine feasibility, financial viability, predicted performance and to optimise system operation.[20] Spectral data are especially relevant, and there is increasing demand for researching new solar technologies.[20] Recent studies show that neglecting spectral and angular details can result in significant deviations in PV power modelling.[21] Therefore, using one standardised spectrum is insufficient for determining cell efficiency.[22] Hence, to define the efficiency of innovative solar energy applications more accurately, the use of local spectral measurements[23,24] or spectral radiation models, such as SMARTS,[1] is proposed.

In the *health* domain, the spectral composition of solar radiation is important for a wide variety of effects, both beneficial and deleterious and the balance of exposure therein. Vitamin D is well known to be induced in the skin by irradiation with UV-B[25]; however, there is increasing focus on the effects of longer wavelength light and overall spectral composition. UV-A in solar radiation induces nitric oxide formation in the skin, leading to a reduction in blood pressure and cardiovascular risk,[26] with non-damaging doses of daylight shown to initiate these effects *in vitro*.[27] Daylight photodynamic therapy relies primarily on blue light[28]; however, a full spectral weighting of biological efficacy is applied to daylight for the most accurate dosimetry.[29] In such applications, a range of measurement methods may be used, even though simpler methods are often desired where dosimeters (e.g. photodiode detectors) can be calibrated to a biological weighting function.

In *daylighting research, design and application*, the spectral characteristics of daylight are simulated to serve the daylighting design process and related research. These simulations are, for example, used to estimate non-image forming (NIF) effects,[30–32] or to assess the appearance of urban environments and building spaces in architecture and lighting visualisations.[15,33,34] For this purpose, several approaches are being used to implement the spectral information in various simulation tools. First of all, spectral measurements in LARK[35] and LUMOS,[36] high dynamic range images for image-based lighting simulations in Radiance,[33] but also spectral sky models, such as the physics-based radiative transfer model libRadtran used in ALFA,[37] or data-driven models,[38,39] and the 'L to CCT' models,[40] of which the latter are used in Radiance[41] and OWL.[42]

For application purposes, the spectral characteristics of daylight are, for example, captured by spectroradiometers, sensors, (fisheye) cameras or dosimeters. These measurements can be used in the quantification of spectral daylight exposure, which is relevant for lighting applications and related research purposes,[43–46] specifically in the estimation of NIF effects,[47–49] photodynamic therapy[28] or advanced lighting control systems.[50,51] SPDs are directly measured[30–32] or derived from chromaticity coordinates of cameras or RGB and XYZ sensors by means of a reconstruction method.[52,53]

Spectral characteristics of daylight have also found their way into *artwork*, where artists use spectral measurements and observations to study and present the colour of the sky in their art.[54–56]

### 1.2 Use of standardised spectral profiles of solar radiation and daylight

CIE and ISO provide standardised SPDs representing daylight known as D Illuminants.[57] These D Illuminants have a notation that reflects the correlated colour temperature (CCT) of the daylight source, for example, D65 is the CIE standardised SPD of daylight with a CCT of 6500 K. D Illuminants at any nominal CCT between 4000 K and 25 000 K can be calculated using a mathematical reconstruction procedure proposed by the CIE,[58] as shown in Figure 1. This procedure is most commonly used in daylight research, design and application, especially to evaluate the NIF effects of daylight.[35,59]

The *electric lighting industry* uses the D Illuminants as reference light sources in the determination of the Colour Rendering Index

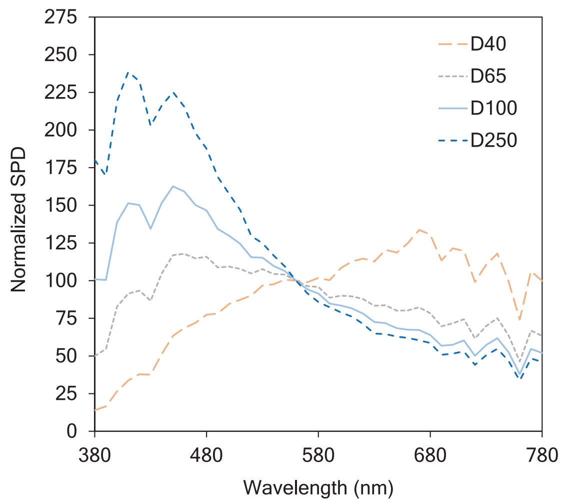


**Figure 1** SPDs derived with the CIE reconstruction procedure for 4000 K (D40), 6500 K (D65), 10 000 K (D100) and 25 000 K (D250)

and the Colour Fidelity Index for all electric light sources with a CCT above 5000 K.[58] Furthermore, D Illuminants are used to define the Television Lighting Consistency Index, a metric to describe the colour rendering qualities of light sources in the *television and broadcasting industry*.[60]

D Illuminants are also used in the field of *museum and artwork* to evaluate damage to artwork through photochemical reaction.[61] In addition, they can support the evaluation of colour *appearance of objects and materials* under daylight.[62–64] Other colour metrics to evaluate the colour quality of materials like colour differences, colour constancy and metamerism used in the graphic arts and printing, paint, coatings, pulp, paper or textile industry, also often employ the standardised D Illuminant.[65,66]

### 1.3 Aim of this paper

As far as the lighting field is concerned, only a small proportion of professionals in daylighting research, design and application use the spectral properties of daylight in their analyses, simulations or product developments.

D Illuminants are primarily used for assessing the quality of objects and light sources under standardised conditions. However, the method used to generate D Illuminants, known as the CIE reconstruction method, is useful in deriving representative SPDs applicable to practical uses in lighting design and research. Hence the aim of this paper is threefold: first, to trace the evolution of the CIE reconstruction method; second, to emphasise the necessity for a localised reconstruction procedure and third, to elaborate on the methodology of data collection and analysis established to develop a localised reconstruction procedure that considers geographical, seasonal and diurnal variations.

## 2. CIE reconstruction method

### 2.1 Historical development

While interest in the spectral characteristics of solar radiation and daylight has increased, this interest has historical precedence. As highlighted by Pissulla *et al.*,[67] the first radiance measurements were published by the scientist C. Dorno in 1911. In 1931, CIE recommended daylight illuminants specified as source B and C for noon sunlight (4800 K) and average daylight (6500 K), respectively, which were positioned just below the Planckian Locus, the locus representing chromaticities of blackbody radiators at different temperatures, which is typically used as reference when addressing the colour of white light.

In the optics and lighting industry, spectral properties of daylight were an important research topic in the 1960s, and several researchers measured spectral characteristics of daylight.[68–71] As described in the Introduction of Judd *et al.*,[72] it was found that both illuminant B and C disregarded the greenish shift of the daylight

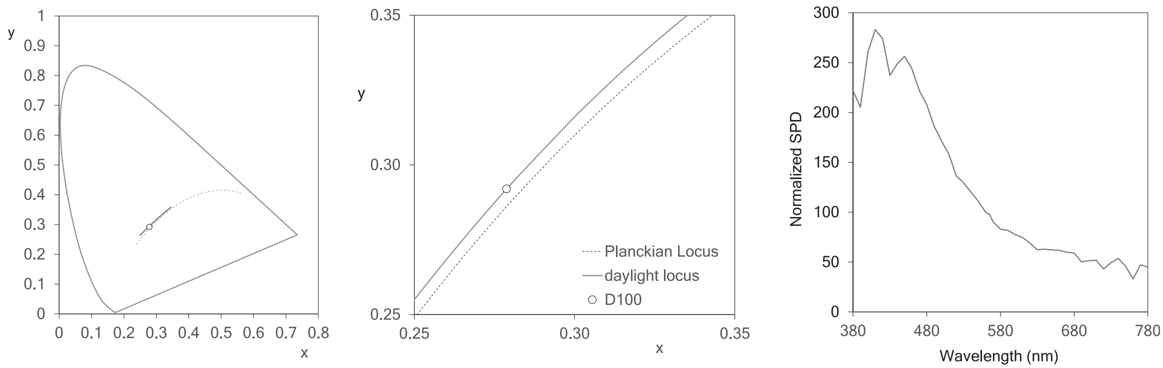


**Figure 2** Daylight characteristics for D100 (D Illuminant for 10 000 K). Left: chromaticity coordinates $x_D$, $y_D$ on the daylight locus for D100; middle: the cut-out of the left image showing chromaticity coordinates, daylight locus and Planckian Locus; right: reconstructed SPD for D100

chromaticities from the Planckian Locus and were perceived as too pink to represent natural daylight (p. 1032). The current representation of the D Illuminants as standardised SPDs representing daylight was initiated by the CIE in 1963.

In a joint activity of the technical colorimetry committees of Canada and the United States,[72] 622 measurement data from Condit and Grum, Henderson and Hodgkiss, and Budde, taken in Ottawa (Canada), Rochester (United States) and Enfield (United Kingdom) respectively,[72] were used to establish a daylight locus and a reconstruction procedure. This daylight locus represents the chromaticities of daylight and lays parallel to, and just above, the Planckian Locus. The established reconstruction procedure can be used to reconstruct the standardised SPDs of daylight (D Illuminants) with one principal vector $S_0$ and two eigenvectors $S_1$ and $S_2$ and their corresponding scalar multiples $M_1$ and $M_2$ for chromaticity coordinates $x_D$ and $y_D$ on the daylight locus. This procedure relies on the correlation between the chromaticity coordinates or CCT of a given daylighting condition and its SPD. Hence, chromaticity coordinates on the daylight locus; thus, a specific CCT corresponds to a single SPD (Figure 2). In the initial release of CIE 15.2 in 1971, the CIE adopted this approach developed by Judd *et al.*[72] with minor adjustments incorporated (for more details, refer to the review by Diakite-Kortlever *et al.*[31] and Figure 3). This approach facilitates the generation of SPDs for D Illuminants from 300 nm to 830 nm, representing spectral daylight distributions accurately enough for colorimetric purposes.[58] For practical use, the reconstruction procedure is integrated, for instance, within the Excel Daylight Series Calculator from the Munsell Color Science Laboratory.[73] This calculator references Wyszecki and Stiles for its implementation.[74]

The CIE reconstruction method is very practical for applications that need SPDs for a CCT bandwidth of daylighting conditions (4000 K to 25 000 K, as defined in Commission International de l'Éclairage[58]), to simulate, predict and estimate the effect of these conditions. In addition, it offers the possibility to reconstruct a representative daylight SPD from chromaticity coordinates and CCT. Therefore, the CIE approach, although not primarily

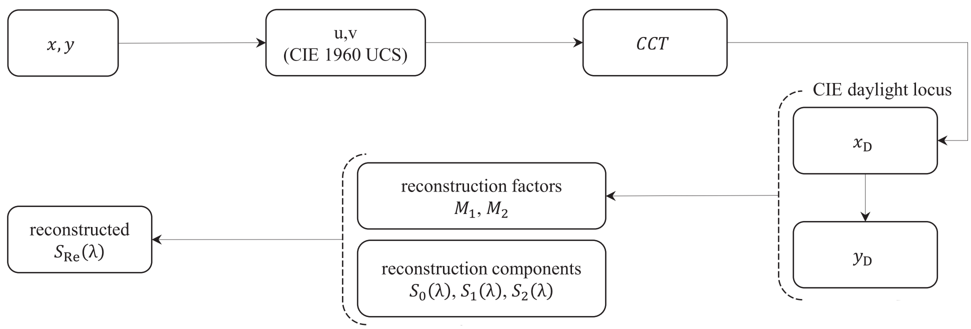


**Figure 3** Approach to reconstruct SPDs ($S_{Re}(\lambda)$) from chromaticity coordinates ($x$, $y$) or CCT
Source: Adopted from Diakite-Kortlever *et al.*,[31] modified.

developed for that purpose, can provide spectral characteristics of daylight from RGB or XYZ sensors, for lighting control solutions and dosimetry,[52,75,76] for spectral simulations in LARK[77] or representations in CCT for lighting design purposes.[59]

## 2.2 Local deviations from D Illuminants

In order to use the CIE reconstruction procedure to derive representative local SPDs of daylight, further development might be required. The 622 measurements taken to establish the CIE reconstruction procedure were conducted in Canada, the United States and the United Kingdom.[72] These datasets have some geographical and climatic similarities, with latitudes between 43° and 52°, continental (Ottawa and Rochester) and maritime (Enfield) climates. To predict NIF effects or colour appearance of building spaces and objects for different locations and seasons, for example, the SPDs of daylight derived with the current CIE reconstruction procedure might not be representative. This is already addressed in ISO/CIE Standard 11664-2 '*Colorimetry – Part 2: CIE Standard Illuminants*',[57] and stated on page 13 in the CIE Technical Report 'Colorimetry' as follows: '*Seasonal and geographical variations in the spectral power distribution of daylight occur, particularly in the ultraviolet spectral region, but this recommendation should be used pending the availability of further information on these variations*'.[58]

Local differences were already found after the publication of Judd *et al.*[72] and the adoption of the procedure by the CIE. Kok, for example, states that, after comparing the SPD of different locations, '*there has been some feeling that the daylight spectral distribution values as accepted by the CIE are too low in the ultraviolet and blue regions of the spectrum*'.[78] Winch *et al.* concluded that '*The evident difference between chromatic conditions in South Africa, and those in the northern hemisphere, raised doubts as to whether the tentative CIE proposals, based on measurements in the northern hemisphere, would apply to conditions in South Africa*'.[79] This is represented in the comparison to the CIE daylight locus: the South African daylight locus is plotted closer to the Planckian Locus (Figure 4(a)). Several researchers derived local daylight loci, as shown in Figure 4, that seem to deviate from the CIE daylight locus.[31,80–85] Most of these daylight loci lay on the green side of the Planckian Locus,[86] some having a lower slope than the Planckian Locus, thus drifting away from the

Planckian Locus at higher CCTs and falling towards the purples for lower CCTs.[68,69,87,88]

Even though a number of researchers confirmed larger differences in the ultraviolet range when compared to reconstructed SPDs according to the CIE reconstruction procedure,[79,80] these differences alone could not have led to a discrepancy in daylight loci, as the daylight locus represents the visible range of the SPD. This range can be from 360 nm to 830 nm; in practical applications, it is often restricted from 380 nm to 780 nm. Thus, local differences within the visible range also might occur, which are relevant for, for example, lighting design, research and application purposes.

The literature indicates that the local differences are likely the result of variations in atmospheric conditions, which are strongly linked to seasonal conditions, with a high impact of the percentage of water vapour in the atmosphere[91]

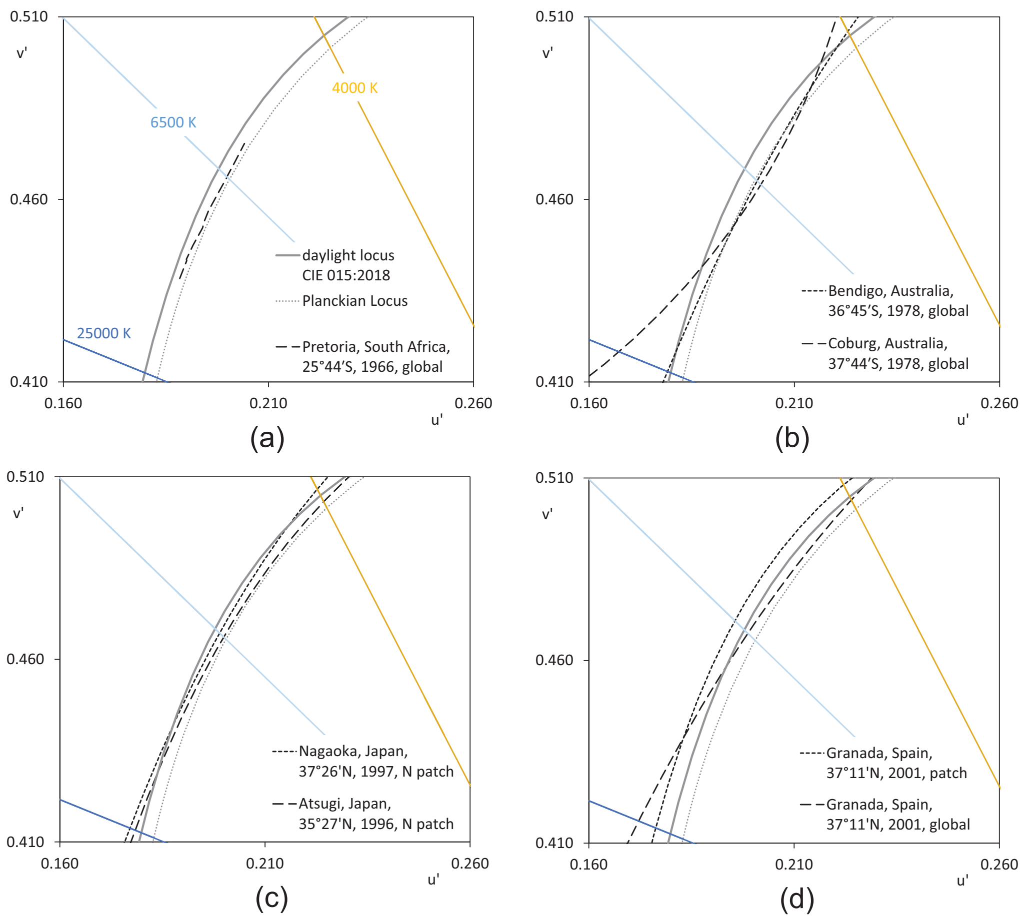


**Figure 4** (continued)

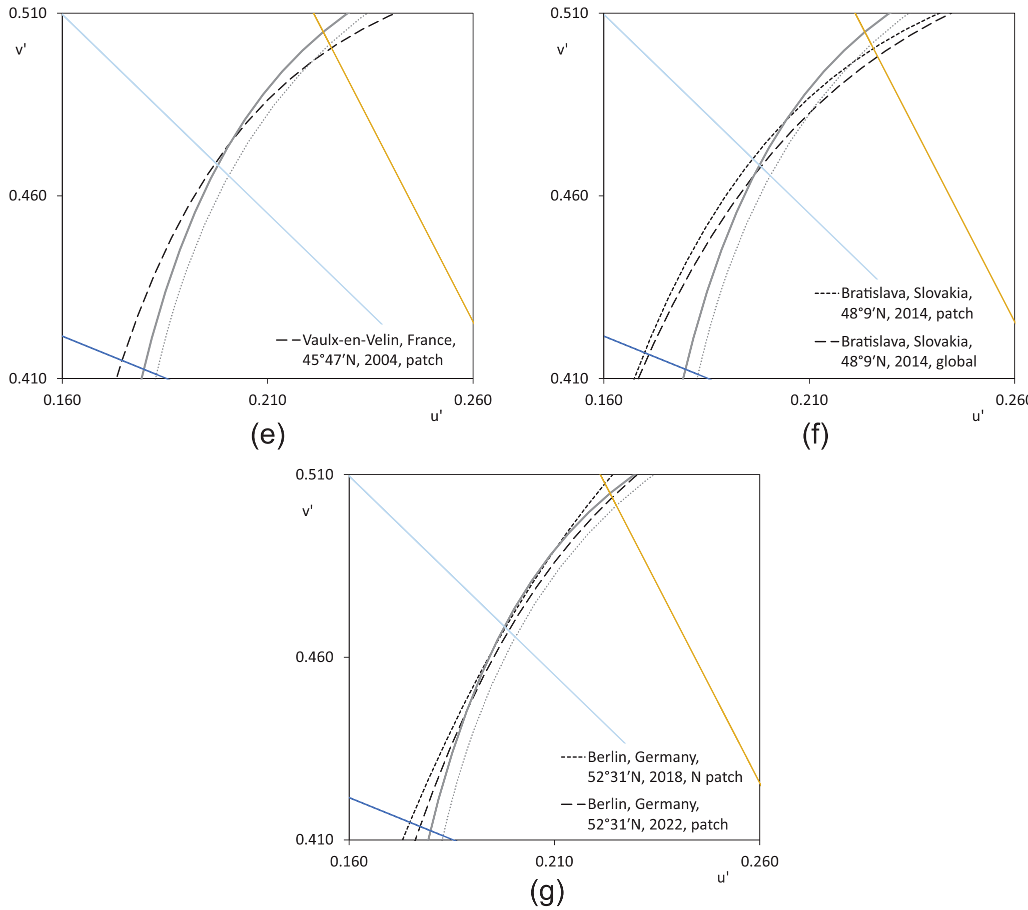


**Figure 4** Local daylight loci in a cut-out of the CIE 1976 uniform chromaticity scale diagram for (a) South Africa,[79] (b) Australia,[80] (c) Japan,[81,82] (d) Spain,[89,90] (e) France,[83] (f) Slovakia[84] and (g) Germany.[31,85] The daylight locus (__), the Planckian Locus (…), as well as iso-temperature lines, referenced in (a), are included for 4000 K and 25 000 K (which correspond to the boundaries outlined in the CIE reconstruction procedure, and represent the typical range of application of daylight loci), and for 6500 K (reference)

and the temperature, thus air pressure.[92] Aerosols, like dust, pollution and industrial particles are said to have little impact.[78,87,88,92,93] This is in contradiction to more recent research that indicates that aerosols are one of the main parameters influencing the variety of spectral distribution of daylight,[18,38] specifically at lower solar altitudes. Spitschan *et al.*[94] found that there is a difference between urban and rural daylighting characteristics during nautical and astronomical twilight (solar altitude $< -6°$), nonetheless pointing out that the urban conditions are being influenced by the presence of electric lighting (light pollution). Ozone concentration will also affect the spectral characteristics of daylight in dusk, dawn and twilight conditions.[18,95,96]

Past research already indicates that in addition to the atmospheric characteristics, ground and canopy reflections might play a role as well,[97,98] although this was not confirmed by the analysis of measurements made in Australia by Dixon.[80] Still, nowadays, ground albedo is one of the main parameters considered in the estimation of spectral solar radiation and has already been implemented in existing models.[18,99]

## 2.3 Impact of atmospheric characteristics

The fact that atmospheric conditions could be responsible for temporal and geographical differences in the spectral properties of daylight was already addressed in the documentation of the reconstruction procedure in the 1960s. In the CIE reconstruction procedure, the primary eigenvector, $S_1$, is linked to variations in the yellow-blue direction. Judd *et al.* observed: '*This variation from yellow to blue generally corresponds to the presence or absence of clouds in the sky, and in the inclusion or exclusion of direct sunlight*'.[72] Moreover, the second eigenvector, $S_2$, implies a green–pink variation, potentially resulting from variations of water in the form of vapour and haze.[72] Several researchers confirmed the yellow–blue and green–pink variations in their reviews of the CIE reconstruction procedure.[80–82,84,87] However, these findings were not substantiated by Hernández-Andrés *et al.*[90] and Diakite-Kortlever *et al.*[31]

To date, the reconstruction procedure has not accounted for atmospheric influences on daylight's spectral characteristics. However, various approaches from different disciplines consider atmospheric properties in determining daylight spectra. For example, the influence of the atmospheric turbidity on the spectral distribution of solar irradiance components was investigated by Kaskaoutis *et al.*[100] They found a wavelength dependence relation between the diffuse-to-global and diffuse-to-direct-beam irradiance ratios with exponential fit, which can be modified as a function of the solar zenith angle and atmospheric turbidity conditions. According to their results, the slope of the curves strongly depended on the processes attenuating irradiance and aerosol optical characteristics in the short wavelengths. Relations were proposed, which allowed the estimation of the spectral distribution of diffuse irradiance as a function of the measured broadband global and diffuse solar irradiances. Differences between rural and urban environments were also found.

## 2.4 Recourse to other disciplines

The CIE reconstruction procedure was adopted and has not been changed over the last 50 years. In the meantime, other disciplines developed approaches that can be used to derive spectral solar data, as mentioned in the introduction:

- Physics-based radiative transfer models, such as libRadtran[6,99]
- Rigorous models, for example MODTRAN,[8] and simplified spectral radiation models, for example SPCTRL2 and SMARTS[1,101]
- Reference solar spectra (total global, direct and diffuse) by the CIE,[102] derived by means of SMARTS[1]
- Analytical fitted sky models, developed with brute force calculation[16–18] or machine learning[39,103]
- Models using approximations with lookup tables[15]

The literature states that the models provide good-to-very good spectral characterisation of daylight under varying conditions, typically requiring detailed information about atmospheric conditions, turbidity or ground albedo. While these models address local differences in spectral characteristics of daylight, limited accessibility to atmospheric data can be a hurdle for professionals working in the field of lighting design, research and application. Despite this challenge, since extensive validation of these models has been conducted, our methodology to verify and modify the CIE reconstruction procedure can rely on utilising predefined atmospheric profiles used in some of these models.

The atmospheric profiles used in libRadtran[99] will be considered here because of their use in the daylighting design simulation tool ALFA to ensure an aligned approach within the lighting community. The predefined atmospheric profiles in libRadtran, which are taken from Anderson *et al.*,[104] contain information about pressure, temperature and concentrations of ozone, oxygen, water vapour, $CO_2$ and $N_2O$. The 1976 US Standard profile is supplemented with region-specific profiles of the US Air Force Geophysics Laboratory (AFGL), differentiating in tropic, mid-latitude and sub-arctic regions.[104] The US Standard profile is being used by Wilkie *et al.*[18] ALFA implemented the standard mid-latitude summer profile, as reported in Balakrishnan.[34]

Predefined aerosol mixtures in libRadtran are taken from Optical Properties of Aerosols and Clouds (OPAC),[105] in which the properties of a mix of aerosols within atmospheric layers as well as combined in the aerosol optical depth over several atmospheric layers are categorised as follows: continental (clean, average and polluted), maritime (clean, polluted and tropical), urban, desert and Antarctic. These OPAC aerosol profiles are also used by Wilkie *et al.*,[18] whereas aerosol information can also be derived from, for example, databases,[20,106] such as the ones from Copernicus[107] and NASA.[108]

To include ground albedo, spectral measurements or openly accessible databases can be considered.[1,20,108] In this process, predefined details with respect to ground albedo as used in libRadtran, mainly defined by the International Geosphere Biosphere Programme (IGBP)[109] will be considered.

## 3. Method for data collection and analysis to review and adjust the CIE reconstruction procedure

Several researchers have proposed locally adapted procedures, and a summary is provided in Diakite-Kortlever *et al.*[31] To establish a comprehensive framework, Technical Committee TC 3-60 (*Spectral daylight characteristics*) of Division 3 (*Interior environment and lighting design*) of the CIE was established. The aim of this committee is to review geographical, seasonal and diurnal variations in daylight's SPD and propose an adjusted CIE reconstruction procedure for deriving representative local spectral distributions of daylight suited for practical applications. This section describes the approach of CIE TC 3-60 and its potential to incorporate future spectral daylight measurements beyond the committee's effort.

### 3.1 Collection of local spectral data

The importance of comprehensive, long-term and worldwide measurements to develop theoretically accurate models for spectral characteristics of daylight has been established by several researchers.[31,77,110]

Hence within the TC 3-60, a worldwide campaign to collect and standardise measurements of spectral characteristics of daylight has been launched. In order to obtain detailed background information on the collection of the measurement data, the TC members describe their measurement site using a template.[110] The majority of TC members work with spectroradiometers, described by the CIE in detail in terms of device characteristics and calibration and use.[111,112] The members also participate in a Round Robin study, an inter-laboratory study of spectral measurement devices that are compared with a reference spectroradiometer (JETI specbos 1211-2, JETI Technische Instrumente GmbH, Jena, Germany). The datasets collected with the reference spectroradiometer at various locations as part of the Round Robin procedure are used to evaluate the individual measuring device deviations. The Round Robin procedure will be described in another paper.

The committee collects spatially resolved (patch) and global (hemispherical) measurements from various locations, both from TC members and publicly available data.[113] Patch measurements include measurements of the spectral radiance of parts of the sky.[5,45,114–116] They offer a wider CCT range and usually do not include direct sunlight. Depending on the position of the patches, the measurements can be more strongly influenced by the composition of the atmosphere. The global horizontal spectral irradiance measurements usually include direct sunlight, and due to their horizontal orientation, they are less influenced by the composition of the atmosphere, especially at higher solar altitudes. In a later phase of the TC's work, it will be investigated whether patch and global measurements provide congruent SPDs.

As the available datasets vary in number per location, data cleaning and selection are performed to create as homogeneous a set of data as possible.[113] As mentioned before, measurements for lower solar altitudes and of lower patch almucantars need separate consideration. As atmospheric influences are in particular to be expected during dusk, dawn and twilight, the measurements are divided into those with a solar altitude below or above 15°, as proposed by Hošek and Wilkie[17] and Knoop *et al.*[110] and considered separately. For datasets of patch measurements, those related to the lower almucantars are analysed separately for the same reason, following the approach in Diakite-Kortlever *et al.*[31]

Also, this work is related to spectral characteristics of daylight for humans (lighting design, research and application, through simulations and measurements), thus with a focus on the visible range of radiation (380 nm to 780 nm, excluding the UV and IR regions).

### 3.2 Initial characterisation of localised spectral data

In order to consider geographical, climatic and atmospheric differences in spectral measurements, characterisation of the locations, as addressed in Section 2.3 will be done using freely available and easily accessible information. Where possible, a finer characterisation has been included for data analysis, although the aim remains to return to the profiles proposed in libRadtran (a coarser characterisation) for planning purposes. Characterisation includes:

- In line with the approach proposed by Lefèvre *et al.*,[117] the locations are assigned an AFGL atmospheric profile[104] as used in libRadtran; tropical (15N), mid-latitude (45N) and sub-arctic (60N),[118] based on the location's latitude. For the purpose of the revision of the CIE reconstruction procedure, CIE TC 3-60 will work the following categorisation: tropical ($\leqslant 23°$), mid-latitude (between 23° and 60°) and sub-arctic ($\geqslant 60°$). Further refinement of the climate is done using the Köppen–Geiger 1-km resolution climate classification maps of Beck *et al.*[119]
- Seasonality is also addressed according to Lefèvre *et al.*,[117] data from November to April is assigned the (boreal) winter or the (austral) summer profile.
- Default aerosol mixtures (continental clean, average and polluted; maritime clean, polluted; tropical; urban; desert and Antarctic,

as defined in Hess *et al.*[105] are provided in libRadtran.[118] These default mixtures are assigned after characterisation according to Li *et al.*[120] The Source Classification Analysis (SCAN) aerosol type classification by Mylonaki *et al.*[121] is also included in Table 1, even though its classification resolution (continental polluted, clean continental, marine and dust) might not be fine enough.

- In addition, the previously discussed measurement site template gives information about the monitoring sites being located in an urban or rural area, which would allow a characterisation with libRadtran profiles by Shettle,[122] and it provides an estimate of the turbidity degree (clean, average, polluted).

All details for the participating CIE TC 3-60 members and additional datasets can be found in Table 1. This categorisation allows, for example, an analysis of the impact of latitude by comparing Berlin, Vaulx-en-Velin and Roskilde, having the same climate (Cfb) and aerosol characteristics (continental clean, weakly polluted). The impact of the season can be studied with data from sites with full-year measurements available, like Beijing, Berlin, Eugene and Vaulx-en-Velin.

## 3.3 Data preparation and analysis

### *3.3.1 Method*

A systematic analysis of the measurement data from the locations listed in Table 1 is planned. This analysis will provide information on geographical, seasonal and diurnal variations and enable local adjustments to be made in the reconstruction procedure and will be covered in more detail in a follow-up publication once the Round Robin has been completed and the data analysis can be finalised.

To illustrate how the reconstruction procedure is being revised, this publication briefly discusses the data preparation and the planned analysis.

All spectral daylight measurements, spectral global horizontal irradiances and spectral patch radiances, are organised in a predefined data frame structure, as described in Balakrishnan *et al.*[113] to allow consistent analysis of the various spectral datasets.

In line with the work of Judd *et al.*,[72] Hernández-Andrés *et al.*[89,90] and Diakite-Kortlever *et al.*[31] the local daylight SPDs will be used in a principal component analysis to establish a revised CIE reconstruction procedure, in which geographical, climatic and seasonal characteristics will be considered as parameters. As the work of Hernández-Andrés *et al.*[123] indicates that the spectral characteristics of daylight worldwide have some basic similarities. Therefore, a reconstruction procedure with variables to account for site characteristics will be developed.

In the evaluation of the quality of the revised reconstruction procedure, measured SPDs are compared with SPDs derived with the:

a. Current CIE reconstruction procedure
b. Revised CIE reconstruction procedure for application, considering geographical, seasonal and diurnal differences
c. libRadtran, using a standard atmospheric profile

For practical and perceptual purposes, the analysis will refer to categories reflecting the CCT both in Kelvin and in Mired, respectively.

The accuracy of the approaches to establish SPDs will be reflected in a goodness-of-fit coefficient (GFC),[124] in line with the approach used by Hernández-Andrés *et al.*[90,125] and Diakite-Kortlever *et al.*[31]

**Table 1** Categorisation of measurement sites of participants in CIE TC 3-60 and external data sources

| Location (country, latitude) | Köppen–Geiger climate classification system* | Allotted AFGL atmospheric profiles | Lower troposphere – (category number)[120] | Proposed aerosol mixtures,[105] based on Li *et al.*[120] | SCANs aerosol mixture classification | Urban/rural, turbidity |
|---|---|---|---|---|---|---|
| Beijing (CHN, 40°) | Dwa | Mid-latitude | 4/7 | Continental average – polluted | Continental – polluted | Urban, average |
| Berlin (DEU, 53°) | Cfb | Mid-latitude | 2 | continental clean | Continental – polluted | Urban, average |
| Bialystok (POL, 53°) | Dfb | Mid-latitude | 2 | Continental clean | Continental – polluted | Urban, average |
| Chilton (UK, 52°) | Cfb | Mid-latitude | 2 | continental clean | Continental – polluted | Rural, average |
| Chongqing (CHN, 30°) | Cfa | Mid-latitude | 7 | Continental polluted | Continental – polluted | No info |
| Dublin (IRL, 53°) | Cfb | Mid-latitude | 6/8 | Maritime polluted | Continental – polluted | Urban, average |
| Eindhoven (NLD, 51°) | Cfb | Mid-latitude | 2 | Continental clean | Continental – polluted | Urban, average |
| Eugene (USA, 44°) | Csb | Mid-latitude | 2 | Continental clean | Continental – polluted | Rural |
| Granada (ESP, 37°) | Csa | Mid-latitude | 2 | Continental clean | Continental – polluted | Urban, average |
| Lausanne (CHE, 47°) | Cfb | Mid-latitude | 2 | Continental clean | Continental – polluted | Urban, clean |
| Naples (ITA, 41°) | Csa | Mid-latitude | 4 | Continental average | Continental – polluted | Urban, average |
| Roskilde (DNK, 56°) | Cfb | Mid-latitude | 2 | Continental clean | Continental – clean | Rural, average |
| São Paulo (BRA, −24°) | Cfa | Mid-latitude | 1/2 | Continental clean – average | Continental – polluted | Rural |
| Seattle (USA, 50°) | Csb | Mid-latitude | 2/0 | Continental clean | Continental – polluted | Urban |
| Singapore (SGP, 1°) | Af | Tropical | 1 | Maritime average | Marine | Urban, average |
| Tokyo (JPN, 36°) | Cfa | Mid-latitude | 4 | Continental average | Marine | Urban |
| Vaulx-en-Velin (FRA, 46°) | Cfb | Mid-latitude | 2 | Continental clean | Continental – polluted | Urban, average |

Af: tropical rainforest; AFGL: US Air Force Geophysics Laboratory; Cfa: temperate, no dry season, hot summer; Cfb: temperate, no dry season, warm summer; Csa: temperate, dry summer, hot summer; Csb: temperate, dry summer, warm summer; Dfb: continental, no dry seasons, warm summer; Dwa: continental, dry winter, hot summer; SCAN: Source Classification Analysis 0: background; 1: aged – biomass burning/biogenic; 2: weakly polluted continental; 4: moderately polluted continental; 6: polluted marine; 7: enhanced polluted Asian; 8: remote marine.

*Locations used in Judd *et al.*[72]: all mid-latitude (boreal); Enfield (latitude: 52°): maritime, Cfb; Rochester (latitude: 43°) and Ottawa (latitude: 45°): Dfb – no information of aerosol characteristics for that time frame available.

To assess the relevance of possible differences for practical applications, the analysis will also include the assessment of:

- Perceptibility of colour differences in the daylight as such, reflected in $\Delta u'v'$
- Colour differences for a range of typical building materials in an urban setting, reflected in $\Delta E^*_{ab}$
- Differences in lighting for NIF responses, reflected in melanopic efficacy of luminous radiation $K_{mel,v}$, as used in Diakite-Kortlever *et al.*[31]

*3.3.2 Exemplary representation and partial evaluation*

This paper includes an exemplary representation of three locations to further substantiate the relevance of this work and to give an impression of the use of this methodology described in this section.

The measurements used were carried out in Eindhoven, Lausanne and Vaulx-en-Velin.[126–128] Detailed information regarding these measurements can be found in Table 2. For comparison purposes, the table also contains information on the Enfield, Rochester and Ottawa sites used for the CIE reconstruction method.[72] Care was taken to ensure that certain geographical, climatic and atmospheric characteristics matched in selecting the sites for the exemplary representation. The latitude of all locations was within the range of locations used for the CIE reconstruction method. Eindhoven shares similar attributes with Vaulx-en-Velin in terms of climate and atmospheric/aerosol properties. Still, it has a different latitude, while Lausanne mirrors the latitude of Vaulx-en-Velin but exhibits different turbidity conditions. Due to the variability in the available datasets, seasonal alignment was not possible in this study. For the location with full-year measurements (Vaulx-en-Velin), a small number of representative days was selected (four seasons, clear and overcast skies – in total six full days of measurements). Horizontal spectral irradiance measurements were conducted on all sites; the Lausanne site measures skylight only, the other sites measure daylight, combining both skylight and sunlight. The data are publicly available through the data package SKYSPECTRA.[113]

The chromaticity coordinates of measurements are plotted in Figure 5. These are used to derive reconstructed SPDs with the CIE procedure, which allows a comparison between measured and reconstructed SPDs. Reconstructed SPDs are normalised at 560 nm by definition, and the measured SPDs are normalised at 560 nm for the purpose of comparison. Exemplary SPDs (reconstructed and measured) are presented in Figure 6, for each location for a comparable CCT (6000 K to 6100 K), and per location for a higher CCT (the minimum CCT of the highest 10% range for that location, see Table 2). The larger CCT range in Lausanne is due to the measurement of skylight only.

The differences between the measured and reconstructed SPDs shown in Figure 6 are visible in the short-wavelength and long-wavelength ranges, particularly for Eindhoven and Lausanne. For illustration purposes only, $\Delta u'v'$, $\Delta E^*_{ab}$ and $\Delta K_{mel,v}$ (in %) were determined according to the approach shown in Figure 7. GFC for the reconstruction procedure was not addressed at this stage, as only exemplary datasets were chosen. Exemplarily, $\Delta E^*_{ab}$ was defined for two different materials, brick and fine-poured concrete, with the reflected SPDs, $S_{Me,r}(\lambda)$ and $S_{Re,r}(\lambda)$, derived with the spectral reflectance characteristics as shown in Figure 8.

The results of this exemplary analysis are given in Table 3.

Assumed colour perception criteria for LEDs can be adapted to daylight, a $\Delta u'v' > 0.0022$

**Table 2** Characteristics of locations providing spectral daylight measurements for exemplary analysis

| Location<br>Latitude, longitude | Climate characteristics: Köppen, AFGL; aerosol category[120] | Local characteristic, turbidity | Time period (selection of days in:) | Time frame and interval | # of datasets | Approximate CCT range (80% of the data) | Mired |
|---|---|---|---|---|---|---|---|
| Eindhoven[126]<br>51°27′N, 5°29′E | Cfb; mid-latitude; weakly Polluted continental | Urban, average | January–March 2020 | Every 6 min between 8 am and 6 pm over several days | 2055 | 5900 K to 8700 K | 115 to 170 |
| Vaulx-en-Velin[127]<br>45°47′N, 4°55′E | Cfb; mid-latitude; weakly polluted continental | Urban, average | March, June, September, December 2016 | Every 1 min, timestamps with solar altitude $\geqslant 15°$ | 2609 | 5600 K to 8700 K | 115 to 179 |
| Lausanne[126]<br>46°32′N, 6°34′E | Cfb; mid-latitude; weakly polluted continental | Urban, clean | August and September 2020 | Every 6 min between 8 am and 6 pm over several days | 1290 | 6100 K to 17 700 K | 56 to 164 |
| Enfield[70,72]<br>51°39′N, −0°5′E | Cfb: mid-latitude (boreal) | Some light and some heavy industry, otherwise residential with some parks | April 1961–March 1962 | Between 9 am and 5 pm, more or less at random | 274 | 4600 K to 40 000 K | 25 to 217 |
| Ottawa[72]<br>45°25′N, −75°41′E | Dfb; mid-latitude (boreal) | Not published | Not published | Not published | 99 | Not published | – |
| Rochester[71,72]<br>43°9′N, −77°37′E | Dfb; mid-latitude (boreal) | Urban | June–July 1962 | Timestamps with solar altitudes 8°, 10°, 15°, 20° 30°, 40° and 70° on five selected days | 249 | 3530 K to 9660 K | 104 to 283 |

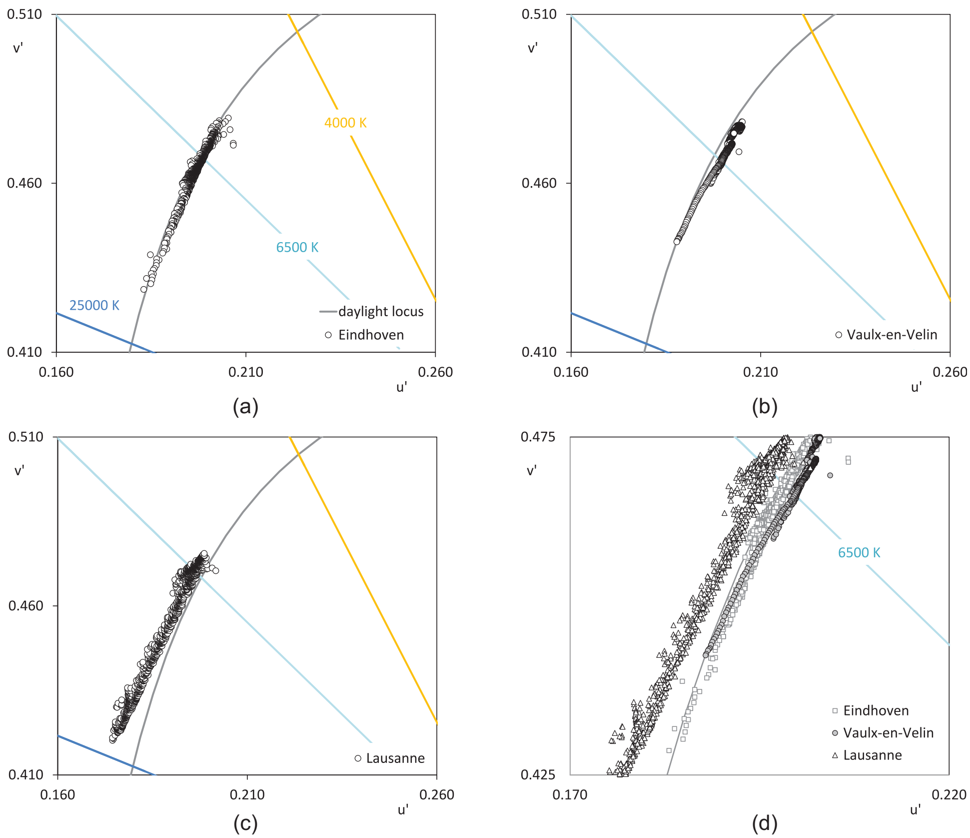


**Figure 5** Chromaticity coordinates of a selection of measurements (solar altitude >15°) for (a) Eindhoven, (b) Vaulx-en-Velin and (c) Lausanne, and all combined (d) in cut-outs of the CIE 1976 uniform chromaticity scale diagram. The daylight locus (__) and iso-temperature lines, referenced in (a), are included for 4000 K and 25 000 K (which correspond to the boundaries outlined in the CIE reconstruction procedure and represent the typical range of application of daylight loci) and for 6500 K (reference)

(representing two-step MacAdam ellipse) is perceptually different.[130–132] Table 3 includes the percentage of the measurements of a dataset that exceeds this value. It shows that there would be very few perceptual differences between reconstructed and measured daylight for Eindhoven and Vaulx-en-Velin, for the chosen set of measurements. For the majority of the Lausanne measurements, there is a perceptual difference between measured and reconstructed daylight. Nonetheless, Table 3 also shows that the reconstructed SPDs in Figure 6 do not lead to a different colour perception of brick and concrete compared to the materials under the measured SPDs. The maximum deviation of $K_{\mathrm{mel,v}}$ in % is given for the SPDs shown in Figure 6, for representation purposes only.

Due to the measurement configuration and the selection of data, the 'high' CCT considered for Lausanne is higher than that of Eindhoven and Vaulx-en-Velin (Table 2). To compensate for this, a reconstructed SPD for Lausanne with a CCT of 8700 K was also considered, resulting in a $\Delta K_{\mathrm{mel,v}}$ of 1.3%.

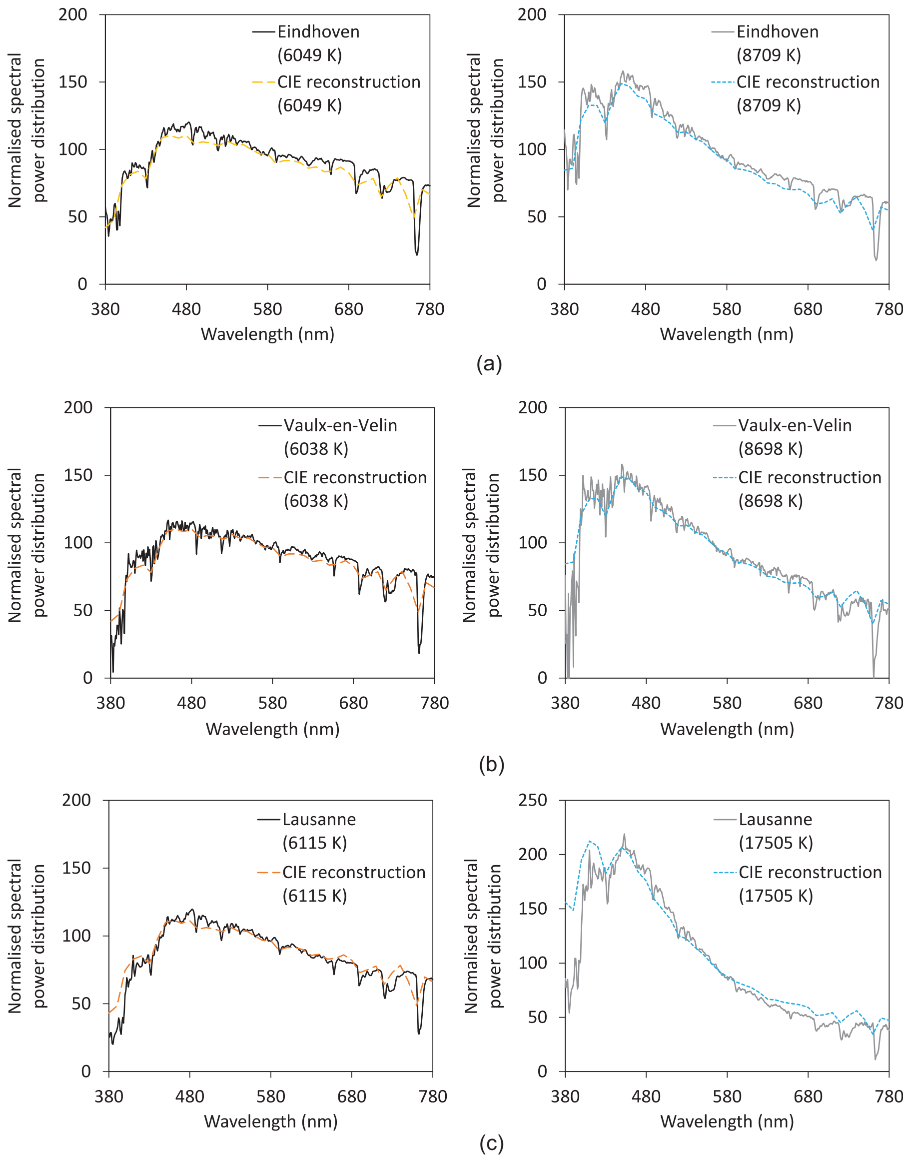


**Figure 6** Exemplary SPDs with a lower (left) and higher (right) CCT respectively, for (a) Eindhoven, (b) Vaulx-en-Velin and (c) Lausanne, including the reconstructed SPDs

It is noteworthy that the analysis is based on horizontal measurements only, in Lausanne measurement of skylight only, in Eindhoven and Vaulx-en-Velin measurements including sunlight. All do not reflect orientation-dependent differences that can be determined with patch measurements, as presented in the work of Diakite-Kortlever and Knoop.[59]

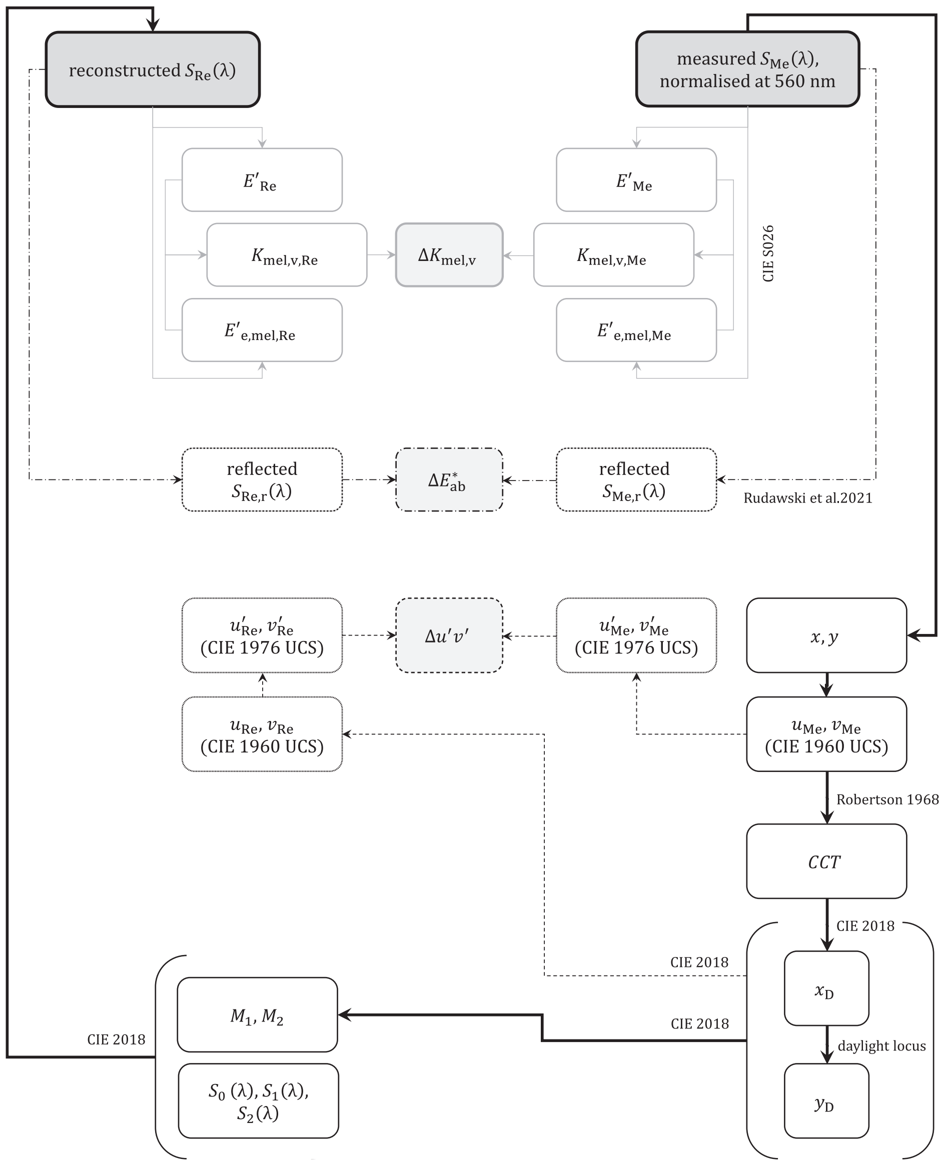


**Figure 7** Diagram of the approach to determine $\Delta u'v'$(— lines), $\Delta E^*_{ab}$ (- - - lines) and $\Delta K_{mel,v}$ (____ lines). Irradiance, $E'_e$, and illuminance $E'$ values are based on normalised SPDs

It should be noted that no conclusions about the validity of the CIE reconstruction method can be drawn from the material presented here. The exemplary SPDs come from locations that lie within the range of the latitude-range of the locations used for the CIE reconstruction method

**Table 3** Results with respect to the perceived difference and NIF effects between the measured and reconstructed values of daylight

| Location | % of measurements with $\Delta u'v' > 0.002$ | $\Delta E^*_{ab}$ – brick | | $\Delta E^*_{ab}$ – concrete | | % of difference in $K_{mel,v}$ for SPDs in Figure 6 for | |
|---|---|---|---|---|---|---|---|
| | | Low CCT | High CCT | Low CCT | High CCT | Low CCT | High CCT |
| Eindhoven | 0.54 | 0.18 | 0.17 | 0.07 | 0.04 | 1.4 | 0.9 |
| Vaulx-en-Velin | 0.36 | 0.19 | 0.14 | 0.07 | 0.01 | 0.6 | 0.2 |
| Lausanne | 99.7 | 0.24 | 0.67 | 0.16 | 0.26 | 0.8 | 1.8 |

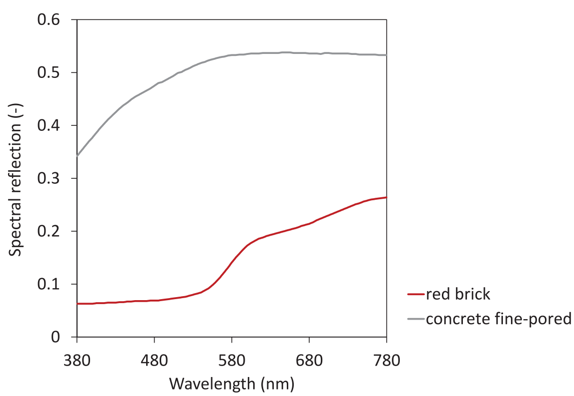


**Figure 8** Spectral reflection for red brick and fine-poured concrete[129]

(see Table 2). Geographical, seasonal and diurnal differences were not addressed in this exemplary analysis.

Future analyses will follow this methodology, considering local, latitudinal or seasonal reconstruction methods in addition to the CIE reconstruction. Quality will be represented in both the application metrics used above and in the GFC.

## 4. Summary and outlook

This paper describes the methodology of data collection and analysis to review and modify the CIE reconstruction procedure to create representative local SPD of daylight for lighting research, planning and application purposes. The work focusses on the visible range of radiation and excludes the UV and IR range. In general, most disciplines that consider UV or IR radiation use models that provide an adequate spectral characterisation of daylight for their application. Although we believe that the lighting field will benefit most from a revised reconstruction method, it could also be useful in other disciplines such as ‘flora and fauna, agriculture and forestry’ and ‘computer graphics’, where a simplified measurement and representation of the visible range of local daylight conditions could be useful. At the same time, the unrevised CIE reconstruction procedure for CIE D Illuminants will be retained in applications that need standardised SPDs for quality and comparison purposes.

To apply the presented methodology and proceed with the data analysis, differences between patch and global horizontal measurements will first be assessed and a Round Robin among participants will be conducted, which will be published at a later stage. The subsequent systematic analysis of the measurement data will allow geographical, seasonal and diurnal adjustments in the reconstruction procedure, if necessary, or confirm the applicability of the unrevised CIE reconstruction method. The work of CIE TC 3-60 will be summarised in a CIE Technical Report.

A locally adapted CIE reconstruction procedure can be used to:

- Set up representative local daylight SPDs for realistic simulations, estimations and predictions
- Provide a simplified measurement and representation of the SPD of daylight
- In turn enable an extension of the global measurement campaign, as it will incorporate RGB and XYZ sensors to collect information on the spectral characteristics of daylight

With this, the lighting research community can further consider:

- The necessity of spatial consideration of spectral characteristics of daylight (e.g. LARK based simulations with horizontal spectral irradiance and uniform colorimetric distribution of sky dome vs. spatially and spectrally resolved sky models, used in ALFA and OWL)
- The validation of spectral sky models[40,113]
- The accuracy of spectral sky models in predicting spectral irradiance in urban settings and indoors[126,133–135]
- The impact of spectral reflectance indoors and outdoors[77,133,136,137]

In the future, this work is intended to support inclusion of spectral characteristics of daylight in standardisation for daylighting design, considering local characterisation.

## Declaration of conflicting interests

The authors declared no potential conflicts of interest with respect to the research, authorship, and/or publication of this article.

## Funding

The authors disclosed receipt of the following financial support for the research, authorship, and/or publication of this article: Most authors received no financial support for the research, authorship and/or publication of this paper. UB financed her works at the Bialystok University of Technology from WZ/WE-IA/3/2023, funded by the research grant from the minister responsible for science in Poland. MM received funding from FNRS – Fonds de la Recherche Scientifique (Belgium), projects SCALE [No. 40000322] and SPARKLE [No. 40024409]. The data from Lausanne and Eindhoven were collected as part of a project that has received funding from the European Union's Horizon 2020 research and innovation programme under the Marie Skłodowska-Curie Grant Agreement No. 75446.

## ORCID iDs

M Knoop https://orcid.org/0000-0002-5097-3623
P Balakrishnan https://orcid.org/0000-0002-2902-1302
UJ Błaszczak https://orcid.org/0000-0003-1967-0365
AK Diakite-Kortlever https://orcid.org/0000-0002-8315-3891
D Dumortier https://orcid.org/0000-0002-3492-4426
J Hernández-Andrés https://orcid.org/0000-0002-6457-7568
M Inanici https://orcid.org/0000-0001-5424-1035
P Kenny https://orcid.org/0000-0002-3598-4703
M Maskarenj https://orcid.org/0000-0001-9546-8236
P O'Mahoney https://orcid.org/0000-0003-3221-5105
C Pierson https://orcid.org/0000-0001-7847-6568
F Rudawski https://orcid.org/0000-0001-6607-5513
A Thorseth https://orcid.org/0000-0003-4344-0770

## References

1 Gueymard CA. The SMARTS spectral irradiance model after 25 years: new developments and validation of reference spectra. *Solar Energy* 2019; 187: 233–253.

2 de Mazière M, Thompson AM, Kurylo MJ, *et al.* The Network for the Detection of Atmospheric Composition Change (NDACC): history, status and perspectives. *Atmospheric Chemistry and Physics* 2018; 18: 4935–4964.
3 Fountoulakis I, Diémoz H, Siani A-M, *et al.* Solar UV irradiance in a changing climate: trends in Europe and the significance of spectral monitoring in Italy. *Environments* 2020; 7: 1.
4 Häder D-P, Lebert M, Schuster M, *et al.* ELDONET – a decade of monitoring solar radiation on five continents. *Photochemistry and Photobiology* 2007; 83: 1348–1357.
5 Riechelmann S, Schrempf M, Seckmeyer G. Simultaneous measurement of spectral sky radiance by a non-scanning multidirectional spectroradiometer (MUDIS). *Measurement Science and Technology* 2013; 24: 125501.
6 Mayer B, Kylling A. Technical note: The libRadtran software package for radiative transfer calculations – description and examples of use. *Atmospheric Chemistry and Physics* 2005; 5: 1855–1877.
7 Ricchiazzi P, Yang S, Gautier C, *et al.* SBDART: a research and teaching software tool for plane-parallel radiative transfer in the earth's atmosphere. *Bulletin of the American Meteorological Society* 1998; 79: 2101–2114.
8 Berk A, Bernstein LS, Robertson DC. MODTRAN: a moderate resolution model for LOWTRAN. Retrieved 9 January 2025 from https://apps.dtic.mil/sti/pdfs/ADA214337.pdf
9 Matsuda R, Ito H, Fujiwara K. Effects of artificially reproduced fluctuations in sunlight spectral distribution on the net photosynthetic rate of cucumber leaves. *Frontiers in Plant Science* 2021; 12: 675810.
10 Durand M, Murchie EH, Lindfors AV, *et al.* Diffuse solar radiation and canopy photosynthesis in a changing environment. *Agricultural and Forest Meteorology* 2021; 311: 108684.
11 Ashdown I. Climate-based annual daylight modelling for greenhouses with supplemental electric lighting. *Acta Horticulturae* 2020; 1296: 583–590.
12 Sánchez-Marañón M, García PA, Huertas R, *et al.* Influence of natural daylight on soil color description: assessment using a color-appearance model. *Soil Science Society of America Journal* 2011; 75: 984–993.
13 Debevec P.Image-based lighting. *Proceedings of SIGGRAPH '06: ACM SIGGRAPH 2006 Courses*, Boston, MA, USA, 30 July to 3 August 2006.
14 Debevec P. Rendering synthetic objects into real scenes: bridging traditional and image-based graphics with global illumination and high dynamic range photography. *Proceedings of the 25th Annual Conference on Computer Graphics and Interactive Techniques (SIGGRAPH '98)*, Orlando, FL, USA, 19–24 July 1998: 189–198.
15 Hillaire S. A Scalable and production ready sky and atmosphere rendering technique. *Computer Graphics Forum* 2020; 39: 13–22.
16 Preetham AJ, Shirley P, Smits B. A practical analytic model for daylight. *SIGGRAPH '99: Proceedings of the 26th Annual Conference on Computer Graphics and Interactive Techniques*, Los Angeles, CA, USA, 8–13 August 1999: 91–100.
17 Hošek L, Wilkie A. An analytic model for full spectral sky-dome radiance. *ACM Transactions on Graphics* 2012; 31: 1–9.
18 Wilkie A, Vevoda P, Bashford-Rogers T, *et al.* A fitted radiance and attenuation model for realistic atmospheres. *ACM Transactions on Graphics* 2021; 40: 1–14.
19 Bruneton E. A qualitative and quantitative evaluation of 8 clear sky models. *IEEE Transactions on Visualization and Computer Graphics* 2016; 23: 2641–2655.
20 Sengupta M, Habte A, Wilbert S, *et al Best Practices Handbook for the Collection and Use of Solar Resource Data for Solar Energy Applications: Third Edition*. NREL/TP-5D00-77635. Golden, CO, USA: National Renewable Energy Lab, 2021. Retrieved 9 January 2025 from https://www.osti.gov/biblio/1778700
21 Lindsay N, Libois Q, Badosa J, *et al.* Errors in PV power modelling due to the lack of spectral and angular details of solar irradiance inputs. *Solar Energy* 2020; 197: 266–278.

22 Kinsey GS, Riedel-Lyngskær NC, Miguel A-A, *et al*. Impact of measured spectrum variation on solar photovoltaic efficiencies worldwide. *Renewable Energy* 2022; 196: 995–1016.

23 University of Oregon Solar Radiation Monitoring Lab. UO SRML Outdoor Spectral Data. Retrieved 9 January 2025 from https://midcdmz.nrel.gov/apps/spectra.pl?UOSMRL

24 Vignola F, Peterson J, Kessler R, *et al*. Improved field evaluation of reference cells using spectral measurements. *Solar Energy* 2021; 215: 482–491.

25 Young AR, Morgan KA, Harrison GI, *et al*. A revised action spectrum for vitamin D synthesis by suberythemal UV radiation exposure in humans in vivo. *Proceedings of the National Academy of Sciences of the United States of America* 2021; 118: e2015867118.

26 Weller RB, Wang Y, He J, *et al*. Does incident solar ultraviolet radiation lower blood pressure? *Journal of the American Heart Association* 2020; 9: e013837.

27 Hazell G, Khazova M, O'Mahoney P. Low-dose daylight exposure induces nitric oxide release and maintains cell viability in vitro. *Scientific Reports* 2023; 13: 16306.

28 Wiegell SR, Haedersdal M, Philipsen PA, *et al*. Continuous activation of PpIX by daylight is as effective as and less painful than conventional photodynamic therapy for actinic keratoses; a randomized, controlled, single-blinded study. *British Journal of Dermatology* 2008; 158: 740–746.

29 O'Mahoney P, Khazova M, Eadie E, *et al*. Measuring daylight: a review of dosimetry in daylight photodynamic therapy. *Pharmaceuticals* 2019; 12: 143.

30 Bellia L, Błaszczak U, Fragliasso F, *et al*. Matching CIE illuminants to measured spectral power distributions: a method to evaluate non-visual potential of daylight in two European cities. *Solar Energy* 2020; 208: 830–858.

31 Diakite-Kortlever AK, Weber N, Knoop M. Reconstruction of daylight spectral power distribution based on correlated color temperature: a comparative study between the CIE approach and localized procedures in assessing non-image forming effects. *LEUKOS* 2023; 19: 118–145.

32 Gkaintatzi-Masouti M, van Duijnhoven J, Aarts MPJ. Review of spectral lighting simulation tools for non-image-forming effects of light. *Journal of Physics: Conference Series* 2021; 2042: 12122.

33 Inanici M. Applications of image based rendering in lighting simulation: development and evaluation of image based sky models. *Proceedings of the 16th IBPSA (International Building Performance Simulation Association) Conference*, Rome, Italy, 2–4 September 2019: 27–30.

34 Balakrishnan P.Measuring and modelling equatorial light. PhD dissertation, University of Technology and Design Singapore, Singapore, 2019.

35 Inanici M, Brennan M, Clark E. Multi-spectral lighting simulations: computing circadian light. *Proceedings of the 14th IBPSA (International Building Performance Simulation Association) Conference*, Hyderabad, India, 7–9 December 2015.

36 Rudawski FR. The spectral radiosity simulation program LUMOS for lighting research applications. *Proceedings LICHT 2023 – 25. European Lighting Congress*, Salzburg, Austria, 26–29 March 2023: 110–115.

37 Solemma. *ALFA – Adaptive Lighting for Alertness*. Retrieved 9 January 2025 from https://www.solemma.com/alfa

38 Kider JT, Knowlton D, Newlin J, *et al*. A framework for the experimental comparison of solar and skydome illumination. *ACM Transactions on Graphics* 2014; 33: 1–12.

39 Del Rocco J, Bourke PD, Patterson CB, *et al*. Real-time spectral radiance estimation of hemispherical clear skies with machine learned regression models. *Solar Energy* 2020; 204: 48–63.

40 Diakite-Kortlever AK, Knoop M. Forecast accuracy of existing luminance-related spectral sky models and their practical implications for the assessment of the non-image-forming effectiveness of daylight. *Lighting Research and Technology* 2021; 53: 657–676.

41 Wienold J, Diakite AK. Making simulations more colorful: extension of gendaylit to create a colored

sky. *17th International Radiance Workshop*, Loughborough, UK, 2018.
42 Maskarenj M, Deroisy B, Altomonte S. A new tool and workflow for the simulation of the non-image forming effects of light. *Energy and Buildings* 2022; 262: 112012.
43 López-Alvarez MA, Hernández-Andrés J, Romero J, *et al*. Using a trichromatic CCD camera for spectral skylight estimation. *Applied Optics* 2008; 47: H31–H38.
44 Tohsing K, Schrempf M, Riechelmann S, *et al*. Validation of spectral sky radiance derived from all-sky camera images – a case study. *Atmospheric Measurement Techniques* 2014; 7: 2137–2146.
45 Uetani Y. Measurement of the all sky spectral radiance distribution using a fisheye camera and principal component analysis. *Proceedings of EuroSun 2014: International Conference on Solar Energy and Buildings*, Aix-les-Bains, France, 16–19 September 2014.
46 Webler FS, Andersen M. Spectral measurement and classification in the era of big data. *CIE x046:2019 Proceedings of the 29th Session of the CIE*, Washington, DC, USA, 14–22 June 2019: 131–136.
47 Kenny P, Mardaljevic J, Hopfe C. The properties of our everyday spectral microclimate. Retrieved 9 January 2025 from http://hdl.handle.net/10197/11056
48 Amirazar A, Azarbayjani M, Molavi M, *et al*. A low-cost and portable device for measuring spectrum of light source as a stimulus for the human's circadian system. *Energy and Buildings* 2021; 252: 111386.
49 Hartmeyer S, Webler FS, Andersen M. Towards a Framework for Light-Dosimetry Studies: Methodological Considerations. *CIE x048:2021 Proceedings of the Conference CIE 2021*, Online (Hosted by NC Malaysia), 27–29 September 2021.
50 Weber N, Knoop M, Völker S. Adaptive tageslichtabhängige Lichtsteuerung für nicht-visuell wirksame Beleuchtung. *Conference Proceedings Licht 2016*, Karlsruhe, Germany, 25–28 September 2016: 229–234.
51 Rudawski FR, Knoop M. Enhanced human centric lighting-Individual automated lighting condition by means of a wearable light dosimeter. *Proceedings of Lux Junior 2019: 14. Internationales Forum für den lichttechnischen Nachwuchs, Dörnfeld/Ilm*, 6–8 September 2019: 1–7.
52 Hernández-Andrés J, Nieves JL, Valero EM, *et al*. Spectral-daylight recovery by use of only a few sensors. *Journal of the Optical Society of America A* 2004; 21: 13–23.
53 Jung B, Inanici M. Measuring circadian lighting through high dynamic range photography. *Lighting Research and Technology* 2019; 51: 742–763.
54 Hemauer C, Keller R. Voyages atmosphériques (Concerning the blueness of the sky). Retrieved 9 January 2025 from https://hemauerkeller.land/en/voyages-atmospheriques/
55 Hemauer C, Keller R. Hemauer and Keller: observing the sky for the next 30 years. Retrieved still working 26 February 2025 from https://arts.cern/hemauer-and-keller-observing-the-sky-for-the-next-30-years/
56 Herzog A. Blue sky or sky blue? Retrieved 9 January 2025 from https://blueskyorskyblue.com/
57 International Organization for Standardization. *Colorimetry – Part 2: CIE Standard Illuminants*. ISO/CIE 11664-2:2022. Geneva, Switzerland: ISO, 2022.
58 Commission International de l'Éclairage. *Colorimetry*. CIE 015:2018. Vienna, Austria: CIE, 2018.
59 Diakite-Kortlever AK, Knoop M. Non-image forming potential in urban settings – an approach considering orientation-dependent spectral properties of daylight. *Energy and Buildings* 2022; 265: 112080.
60 EBU. R 137: Television Lighting Consistency Index-2012 and Television Luminaire Matching Factor-2013, 2016. Retrieved 9 January from https://tech.ebu.ch/docs/r/r137.pdf
61 Cuttle C. Lighting works of art for exhibition and conservation. *Lighting Research and Technology* 1988; 20: 43-53.
62 Foster DH, Nascimento SMC, Amano K, *et al*. Spatial distributions of local illumination color

in natural scenes. *Vision Research* 2016; 120: 39–44.

63 Chiao CC, Cronin TW, Osorio D. Color signals in natural scenes: characteristics of reflectance spectra and effects of natural illuminants. *Journal of the Optical Society of America A* 2000; 17: 218–224.

64 Chiao CC, Osorio D, Vorobyev M, *et al*. Characterization of natural illuminants in forests and the use of digital video data to reconstruct illuminant spectra. *Journal of the Optical Society of America A* 2000; 17: 1713–1721.

65 Hirschler R, Zwinkels J.Appendix 3: Use of CIE colorimetry in the pulp, paper, and textile industries. In Schanda J, editor, *Colorimetry: Understanding the CIE System*. John Wiley & Sons, Inc., Hoboken, NJ, 2007: 411–428.

66 American Society for Testing and Materials. *D2244 Standard Practice for Calculation of Color Tolerances and Color Differences from Instrumentally Measured Color Coordinates*. West Conshohocken, PA: ASTM, 2022.

67 Pissulla D, Seckmeyer G, Cordero RR, *et al*. Comparison of atmospheric spectral radiance measurements from five independently calibrated systems. *Photochemical & Photobiological Sciences* 2009; 8: 516–527.

68 Nayatani Y, Wyszecki G. Color of daylight from north sky. *Journal of the Optical Society of America* 1963; 53: 626–629.

69 Chamberlin GJ, Lawrence A, Belbin AA. Observations on the related colour temperature of north daylight in southern England. *Light* 1963; 56: 70–72.

70 Henderson ST, Hodgkiss D. The spectral energy distribution of daylight. *British Journal of Applied Physics* 1963; 14: 125–131.

71 Condit HR, Grum F. Spectral energy distribution of daylight. *Journal of the Optical Society of America* 1964; 54: 937–944.

72 Judd DB, MacAdam DL, Wyszecki G, *et al*. Spectral distribution of typical daylight as a function of correlated color temperature. *Journal of the Optical Society of America* 1964; 54: 1031–1040.

73 Munsell Color Science Laboratory. Excel Daylight Series Calculator. Retrieved 9 January 2025 from http://www.rit-mcsl.org/UsefulData/DaylightSeries.xls

74 Wyszecki G, Stiles WS. *Color Science: Concepts and Methods, Quantitative Data and Formulae*. John Wiley and Sons, Inc., Hoboken, NJ, 2000.

75 Botero-Valencia J-S, Valencia-Aguirre J, Durmus D, *et al*. Multi-channel low-cost light spectrum measurement using a multilayer perceptron. *Energy and Buildings* 2019; 199: 579–587.

76 Trinh VQ, Babilon S, Myland P, *et al*. Processing RGB color sensors for measuring the circadian stimulus of artificial and daylight light sources. *Applied Sciences* 2022; 12: 1132.

77 Inanici M. Tristimulus color accuracy in image-based sky models: simulating the impact of sky spectra on daylit interiors. *Proceedings of Building Simulation 2019: 16th IBPSA International Conference and Exhibition*, Rome, Italy, 2–4 September 2019.

78 Kok CJ. Spectral irradiance of daylight at Pretoria. *Journal of Physics D: Applied Physics* 1972; 5: 1513–1520.

79 Winch GT, Boshoff MC, Kok CJ, *et al*. Spectroradiometric and colorimetric characteristics of daylight in the southern hemisphere: Pretoria, South Africa. *Journal of the Optical Society of America* 1966; 56: 456–464.

80 Dixon ER. Spectral distribution of Australian daylight. *Journal of the Optical Society of America* 1978; 68: 437–450.

81 Kobayashi K, Ikemori T, Kawakami G. Spectral distribution of north sky daylight: measurement and reconstitution of spectral distribution. *J-Global* 1997; 81: 983–990.

82 Kobayashi K, Kawakami G, Okuma Y, *et al*. Spectral distribution of north sky daylight at Atsugi. *Journal of the Illuminating Engineering Institute of Japan* 1996; 80: 550–553.

83 Chain C. Caractérisation Spectrale Et Directionnelle De La Lumière Naturelle: Application À L'éclairage Des Bâtiments. *PhD dissertation, ENTPE, Laboratoire des Sciences de l'Habitat, Département Génie Civil et Bâtiment, Vaulx-en-Velin, France*, 2004.

84 Rusnák A. Meranie a Hodnotenie Spektrálnych Charakteristík Slnečného Žiarenia [Measurements and evaluation of spectral sun radiation characteristics]. *PhD dissertation, University of Technology in Bratislava, Faculty of Electrical Engineering and Information Technology, Slovakia*, 2014.

85 Diakite AK, Weber N, Rockstädt E, *et al*. Optimierung des Verfahrens zur Rekonstruktion von Tageslichtspektren aus Farbörter auf dem Daylight Locus. *Proceedings of LICHT 2018*, Davos, Switzerland, 9–12 September 2018.

86 Hisdal V. Spectral distribution of global and diffuse solar radiation in Ny-Ålesund, Spitsbergen. *Polar Research* 1987; 5: 1–27.

87 Sastri VDP, Das SR. Typical spectral distributions and color for tropical daylight. *Journal of the Optical Society of America* 1968; 58: 391–398.

88 Tarrant AWS. The spectral power distribution of daylight. *Lighting Research and Technology* 1968; 33: 75–82.

89 Hernández-Andrés J, Romero J, Lee RL. Colorimetric and spectroradiometric characteristics of narrow-field-of-view clear skylight in Granada, Spain. *Journal of the Optical Society of America A* 2001; 18: 412–420.

90 Hernández-Andrés J, Romero J, Nieves JL, *et al.* Color and spectral analysis of daylight in southern Europe. *Journal of the Optical Society of America A* 2001; 18: 1325–1335.

91 Hull JN. Spectral distribution of radiation from sun and sky. *Lighting Research and Technology* 1954; 19: 21–28.

92 Awadalla NS, Alnaser WE. Solar spectrum distribution and optical depth of Bahrain's sky. *Earth Moon Planet* 1993; 60: 251–264.

93 Sastri VDP. Locus of daylight chromaticities in relation to atmospheric conditions. *Journal of Physics D: Applied Physics* 1976; 9: L1–L3.

94 Spitschan M, Aguirre GK, Brainard DH, *et al.* Variation of outdoor illumination as a function of solar elevation and light pollution. *Scientific Reports* 2016; 6: 26756.

95 Hulburt EO. Explanation of the brightness and color of the sky, particularly the twilight sky. *Journal of the Optical Society of America* 1953; 43: 113–118.

96 Peyvandi S, Hernández-Andrés J, Olmo FJ, *et al*. Colorimetric analysis of outdoor illumination across varieties of atmospheric conditions. *Journal of the Optical Society of America* 2016; 33: 1049–1059.

97 Das SR, Sastri VDP. Spectral distribution and color of tropical daylight. *Journal of the Optical Society of America* 1965; 55: 319–323.

98 Olesen T. Daylight spectra (400–740 nm) beneath sunny, blue skies in Tasmania, and the effect of a forest canopy. *Australian Journal of Ecology* 1992; 17: 451–461.

99 Emde C, Buras-Schnell R, Kylling A, *et al*. The libRadtran software package for radiative transfer calculations (version 2.0.1). *Geoscientific Model Development* 2016; 9: 1647–1672.

100 Kaskaoutis DG, Kambezidis HD, Jacovides CP, *et al*. Modification of solar radiation components under different atmospheric conditions in the Greater Athens Area, Greece. *Journal of Atmospheric and Solar-Terrestrial Physics* 2006; 68: 1043–1052.

101 Gueymard CA. SMARTS2: a simple model of the atmospheric radiative transfer of sunshine: algorithms and performance assessment, 1995. Retrieved 9 January 2025 from https://www.instesre.org/GCCE/SMARTS2.pdf

102 Commission International de l'Éclairage. *Recommended Reference Solar Spectra for Industrial Applications*. CIE 241:2020. Vienna, Austria: CIE, 2020.

103 Satilmis P, Bashford-Rogers T, Chalmers A, *et al*. A Machine-learning-driven sky model. *IEEE Computer Graphics and Applications* 2017; 37: 80–91.

104 Anderson GP, Clough SA, Kneizys FX, *et al.* AFGL atmospheric constituent profiles (0.120 km). Environmental research papers, 1986.

105 Hess M, Koepke P, Schult I. Optical properties of aerosols and clouds: the software package OPAC. *Bulletin of the American Meteorological Society* 1998; 79: 831–844.
106 Papachristopoulou K, Fountoulakis I, Gkikas A, *et al*. 15-Year analysis of direct effects of total and dust aerosols in solar radiation/energy over the Mediterranean basin. *Remote Sensing* 2022; 14: 1535.
107 Copernicus. Atmosphere Data Store. Retrieved 9 January 2024 from https://ads.atmosphere.copernicus.eu/#!/home
108 NASA. MODIS Moderate Resolution Imaging Spectroradiometer. Retrieved 9 January 2024 from https://modis.gsfc.nasa.gov/
109 National Center for Atmospheric Research Staff. The climate data guide – CERES: IGBP land classification. Retrieved 9 January 2024 from https://climatedataguide.ucar.edu/climate-data/ceres-igbp-land-classification
110 Knoop M, Weber N, Diakite AK. Approach to analyse seasonal and geographical variations in daylight illuminants. *CIE x046:2019 Proceedings of the 29th Session of the CIE*, Washington, DC, USA, 14–22 June 2019.
111 Commission International de l'Éclairage. *Spectroradiometric Measurement of Optical Radiation Sources*. CIE 250:2022. Vienna, Austria: CIE, 2022.
112 Commission International de l'Éclairage. *Calibration, Characterization and Use of Array Spectroradiometers*. CIE 233:2019. Vienna, Austria: CIE, 2019.
113 Balakrishnan P, Diakite-Kortlever AK, Dumortier D, *et al*. SKYSPECTRA: an opensource data package of worldwide spectral daylight. *CIE x050:2023 Proceedings of 30th Session of the CIE*, Ljubljana, Slovenia, 15–23 September 2023.
114 Luo T, Yan D, Lin R, *et al*. Sky-luminance distribution in Beijing. *Lighting Research and Technology* 2015; 47: 349–359.
115 Knoop M, Diakite AK, Rudawski FR.Methodology to create spectral sky models to enable the inclusion of colorimetric characteristics of daylight in research and design. *CIE 216:2015 Proceedings of the 28th Session of the CIE*, Manchester, UK, 28 June to 4 July 2015.
116 Dubnicka R, Rusnák A, Komar L, *et al*. Spectroradiometric analysis of sky types according to CIE document CIE S 011/E:2003. CIE x039:2014 *Proceedings of CIE 2014 Lighting Quality & Energy Efficiency*, Kuala Lumpur, Malaysia, 23–26 April 2014.
117 Lefèvre M, Oumbe A, Blanc P, *et al*. McClear: a new model estimating downwelling solar radiation at ground level in clear-sky conditions. *Atmospheric Measurement Techniques* 2013; 6: 2403–2418.
118 Mayer B, Kylling A, Emde C, *et al*. LibRadtran user's guide: edition for LibRadtran version 2.0.4, 2012. Retrieved 9 January 2025 from http://libradtran.org/doc/libRadtran.pdf
119 Beck HE, Zimmermann NE, McVicar TR, *et al*. Present and future Köppen–Geiger climate classification maps at 1-km resolution. *Scientific Data* 2018; 5: 180214.
120 Li J, Hendricks J, Righi M, *et al*. An aerosol classification scheme for global simulations using the K-means machine learning method. *Geoscientific Model Development* 2022; 15: 509–533.
121 Mylonaki M, Giannakaki E, Papayannis A, *et al*. Aerosol type classification analysis using EARLINET multiwavelength and depolarization lidar observations. *Atmospheric Chemistry and Physics* 2021; 21: 2211–2227.
122 Shettle EP. Models of aerosols, clouds, and precipitation for atmospheric propagation studies. *AGARD Conference Proceedings No. 454*, Copenhagen, Denmark, 9–13 October 1989.
123 Hernández-Andrés J, Lee RL, Romero J. Calculating correlated color temperatures across the entire gamut of daylight and skylight chromaticities. *Applied Optics* 1999; 38: 5703–5709.
124 Romero J, García-Beltrán A, Hernández-Andrés J. Linear bases for representation of natural and artificial illuminants. *Journal of the Optical Society of America* 1997; 14: 1007.
125 Hernández-Andrés J, Romero J, García-Beltrán A, *et al*. Testing linear models on spectral

daylight measurements. *Applied Optics* 1998; 37: 971–977.

126 Pierson C, Aarts MPJ, Andersen M. Validation of spectral simulation tools for the prediction of indoor daylight exposure. *Proceedings Building Simulation 2021: 17th Conference of IBPSA*, Bruges, Belgium, 1–3 September 2021.

127 Tourasse G. *Mesure Et Analyse Statistique Tout Temps Du Spectre Du Rayonnement Solaire*. PhD dissertation, Université de Lyon, Lyon, France, 2016: 2.

128 Tourasse G, Dumortier D. Development of a system measuring the solar radiation spectrum in 5 planes for daylight and PV applications. *Energy Procedia* 2014; 57: 1110–1119.

129 Rudawski F, Aydınlı S, Broszio K. Spectral reflectance and transmittance of various materials. 2021 Retrieved 26 February 2025. from https://doi.org/10.14279/depositonce-11893.2.

130 Harbers G, McGroddy K, Petluri R, *et al*. Visual color matching of LED and tungsten-halogen light sources. *CIE x035:2010 Proceedings of CIE 2010 Lighting Quality & Energy Efficiency*, Vienna, Austria, 14–17 March 2010.

131 Narendran N, Deng L, Freyssinier JP, *et al*. Developing color tolerance criteria for white LEDs. Retrieved 9 January 2025 from https://www.lrc.rpi.edu/programs/solidstate/cr_colortoleance.asp

132 Commission International de l'Éclairage. *Chromaticity Difference Specification for Light Sources*. CIE TN 001:2014. Vienna, Austria: CIE, 2014.

133 Balakrishnan P, Jakubiec AJ. Spectral rendering with daylight: a comparison of two spectral daylight simulation platforms. *Proceedings of the 16th IBPSA (International Building Performance Simulation Association) Conference*, Rome, Italy, 2–4 September 2019.

134 Alight A, Jakubiec AJ. Evaluating the use of photobiology-driven alertness and health measures for circadian lighting design. *Proceedings Building Simulation 2021: 17th Conference of IBPSA*, Bruges, Belgium, 1–3 September 2021.

135 Orman A, Safranek S, Pierson C.Implementation of a reconstructed spectral sky definition in a light simulation tool and comparison to measurements. *CIE x050:2023 Proceedings of 30th Session of the CIE*, Ljubljana, Slovenia, 15–23 September, 2023.

136 Bellia L, Pedace A, Fragliasso F. Indoor lighting quality: effects of different wall colours. *Lighting Research and Technology* 2017; 49: 33–48.

137 Kenny P. Characterising the melanopic/spectral microclimate of indoor spaces. *PhD dissertation, Loughborough University, Loughborough, UK*, 2021.